International Journal of Biometeorology (2023) 67:1017–1030
https://doi.org/10.1007/s00484-023-02475-7

ORIGINAL PAPER

The effects of intrinsic water-use efficiency and climate on wood anatomy

Yixue Hong[1,2] · Xiaohong Liu[1,3] · J. Julio Camarero[4] · Guobao Xu[3] · Lingnan Zhang[1] · Xiaomin Zeng[1] · Amy Ny Aina Aritsara[5] · Yu Zhang[1] · Wenzhi Wang[6] · Xiaoyu Xing[7] · Qiangqiang Lu[1,8]

Received: 7 June 2022 / Revised: 5 April 2023 / Accepted: 11 April 2023 / Published online: 18 April 2023

Abstract

Climate warming may induce growth decline in warm-temperate areas subjected to seasonal soil moisture deficit, whereas increasing atmospheric CO_2 concentration (C_a) is expected to enhance tree growth. An accurate understanding of tree growth and physiological processes responding to climate warming and increasing C_a is critical. Here, we analyzed tree-ring stable carbon isotope and wood anatomical traits of *Pinus tabuliformis* from Qinling Mountains in China to understand how lumen diameter (LD) determining potential hydraulic conductivity and cell-wall thickness (CWT) determining carbon storage responded to climate and C_a. The effects of climate and C_a on intrinsic water-use efficiency (iWUE) were isolated, and iWUE values due to only-climate ($iWUE_{Clim}$) and only-CO_2 effects ($iWUE_{CO2}$) were obtained. During a low-iWUE period, the influences of climate on earlywood (EW) LD and latewood (LW) CWT prevailed. During a high-iWUE period, CO_2 fertilization promoted cell enlargement and carbon storage but this was counteracted by a negative influence of climate warming. The limiting direct effects of $iWUE_{Clim}$ and indirect effects of climate on EW LD were greater than on LW CWT. *P. tabuliformis* in temperate forests will face a decline of growth and carbon fixation, but will produce embolism-resistant tracheids with narrow lumen responding to future hotter droughts.

Keywords CO_2 fertilization · Climate warming · Drought · Tree ring $\delta^{13}C$ · Wood anatomy · Temperate forest

✉ Xiaohong Liu
xhliu@snnu.edu.cn

1 School of Geography and Tourism, Shaanxi Normal University, Xi'an 710119, China

2 State Key Laboratory of Biocontrol, School of Ecology, Shenzhen Campus of Sun Yat-Sen University, Shenzhen 518107, China

3 State Key Laboratory of Cryospheric Science, Northwest Institute of Eco-Environment and Resources, Chinese Academy of Sciences, Lanzhou 730000, China

4 Instituto Pirenaico de Ecología (IPE-CSIC), Zaragoza 50092, Spain

5 State Key Laboratory for Conservation and Utilization of Subtropical Agro-Bioresources, Guangxi University, Nanning 530004, China

6 The Key Laboratory of Mountain Environment Evolution and Regulation, Institute of Mountain Hazards and Environment, Chinese Academy of Sciences, Chengdu 610041, China

7 Qinling National Botanical Garden, Xi'an 710061, China

8 Xi'an Botanical Garden of Shaanxi Province (Institute of Botany of Shaanxi Province), Xi'an 710061, China

Introduction

Leaf stomata balance the carbon assimilation of photosynthesis and water loss during transpiration, thus determining carbon and water cycle in forests (Giguere-Croteau et al. 2019; Wang et al. 2021). On the one hand, climate warming with increasing drought stress has a negative effect on tree growth, increasing the risk of growth decline and tree mortality (Allen et al. 2010, 2015), notably for semi-arid forests in warm-temperate areas (Liu et al. 2013a; Drake et al. 2015). On the other hand, the concentration of CO_2 in the atmosphere (C_a) has continuously increased from ~ 277 ppm in 1750 (Joos and Spahni 2008) to 421.4 ppm in 2023 (data from Global Monitoring Laboratory, https://gml.noaa.gov/ccgg/mbl/crvfit/crvfit.html). The ongoing increase of C_a is expected to reverse the negative effect caused by global warming on trees by enhancing growth or by improving intrinsic water-use efficiency (iWUE), i.e., the ratio between photosynthetic rate (A) and the stomatal conductance of water vapor (g_s), through the so-called CO_2 fertilization effect (Pan et al. 2011; Schimel et al. 2015).

Tree-ring studies provide the opportunity to explore the response of tree radial growth to climate warming and rising C_a because tree-ring stable carbon isotope ratios ($\delta^{13}C$) provide information about the tree physiological processes of carbon gain and leaf water loss over long-term scales (Liu et al. 2019; Wang et al. 2021). Increased C_a promotes the metabolic activity of the RuBisco enzyme, which increases A (Huang et al. 2007). Meanwhile, the leaf stomata of C_3 plants tend to close in response to elevated C_a, thus reducing water loss, which leads to a decrease in g_s and intercellular CO_2 concentration (C_i) (Battipaglia et al. 2013) and to an increase iWUE (McCarroll and Loader 2004). Therefore, the long-term variations of iWUE can be estimated through the determination of tree-ring $\delta^{13}C$ (Saurer et al. 2004; Frank et al. 2015; Wang et al. 2021). Recently, increases in iWUE have been found in several forests around the world (Peñuelas et al. 2011; Kannenberg et al. 2021; Saurer et al. 2014). Although some studies have reported that increased tree growth benefited from CO_2 fertilization (e.g., Lu et al. 2018; Wang et al. 2018), most studies concluded that iWUE did not translate into growth enhancement (e.g., Mediterranean areas Andreu-Hayles et al. 2011; González Muñoz et al. 2015; Brito et al. 2016), humid subtropical, temperate, and tropical areas (Nock et al. 2011; Li et al. 2017, 2019)). Particularly, several studies concerning temperate forests subjected to seasonal soil moisture deficit found that improved iWUE did not necessarily lead to growth increases owing to the complex response of trees to drought stress (Peñuelas et al. 2008; Levesque et al. 2014; Frank et al. 2015; Fernández-de-Uña et al. 2016; Giguere-Croteau et al. 2019; Marchand et al. 2020; Belmecheri et al. 2021; Heilman et al. 2021). The lack of growth enhancement may be related to warming-induced drought stress and its interaction with rising CO_2 levels (Andreu-Hayles et al. 2011; Gagen et al. 2011). Yet, tree growth in response to elevated CO_2 concentration and the dynamic interaction between atmospheric CO_2 and warming climate trends remain unclear, especially in temperate forests subjected to episodic seasonal droughts.

To date, either tree-ring width or basal area increment (BAI) are used as proxies of tree growth in most dendrochronological studies exploring CO_2 fertilization (Soulé et al. 2015; Wieser et al. 2018; Liu et al. 2019). In addition to tree-ring width analysis, xylem anatomical traits are potential proxies to reflect the key functions and ecophysiological processes of trees, because some anatomical variables (e.g., lumen diameter (LD), cell wall thickness (CWT)) are strongly related to radial growth, hydraulic conductivity, and carbon allocation (Fonti et al. 2010; Camarero et al. 2015; Cuny et al. 2015; Pellizzari et al. 2016; Castagneri et al. 2020). For example, trees invest more carbon to form embolism-resistant conduits with small conduit diameter and thick cell-wall in response to drought (Hacke et al. 2015). The formation of large conduits with wide lumen and thin walls is also observed during drought and leads to higher hydraulic conductivity, but these conduits are more vulnerable to embolism (Eilmann et al. 2009). Thus, LD and CWT are important indicators for the assessment of tree growth dynamics and forest carbon cycling (Cuny et al. 2015; Fonti and Babushkina 2016; Castagneri et al. 2020). In conifer tree rings, earlywood (EW) and latewood (LW) are formed in the early and late growing seasons, respectively. Thus, wood formation processes (e.g., cell enlargement, cell wall thickening, and maturation) are affected by seasonal climate conditions (Fritts 1976; Vaganov et al. 2006; Castagneri et al. 2017). However, how the interactive effects of CO_2 and climate variation impact on EW and LW anatomical characteristics and their related hydraulic function and carbon allocation is still poorly understood.

The Qinling Mountains are located in central China and represent the transitional climate boundary between the subtropical and temperate zone in China meaning that Qinling Mountains play a major role in Chinese geographical and climatic patterns, biota divisions and natural resources distribution (Ma et al. 2019). Qinling Mountains is a typical climate and ecology-sensitive area. Since the 1960s, there has been a warming and drying trend in these areas, especially a climate shift since the 1990s (Gao et al. 2018) which has greatly influenced regional tree growth. Warming and drying climate and episodic seasonal drought events have caused the decline of conifers due to drought stress in the Qinling Mountains (Liu et al. 2013b, 2018). Here, we put forward that a combination of tree-ring xylem anatomy measurements and iWUE estimate from *Pinus tabuliformis* in the Qinling Mountains can provide an insight into possible CO_2 fertilization effects from an ecophysiological point of view. We analyze tree-ring xylem anatomy characteristics influencing tree-ring width, hydraulic conductivity, and carbon allocation, and quantify iWUE which reflects the balance between carbon assimilation and water vapor loss. We aim to explore how CO_2 fertilization and climate variability and their interaction affect tree-ring anatomy because it is critical for the sustainable management of threatened or protected temperate conifer forests. We hypothesized that the fertilization effect caused by increasing atmospheric CO_2 concentration could not compensate the inhibiting effect caused by climate warming on xylem anatomy characteristics.

Materials and methods

Study area

The western Qinling Mountains are mainly influenced by the east Asian monsoon, characterized by cold and dry climate conditions in winter, but warm and humid conditions in summer. The intra-annual climate performs simultaneous

rain and heat and negative water balance in spring and summer (Fig. S1).

Pinus tabuliformis is one of the dominant tree species in the western Qinling Mountains. We conducted the field sampling in Zhangjiazhuang forest farm (ZJZ, 34° 08′ N, 106° 31′ E, 1,400 m a.s.l.), western Qinling Mountains. The mean annual temperature of ZJZ is 11.6 °C, with monthly means ranging from − 0.4 °C in January to 22.7 °C in July, and the mean annual precipitation is 627 mm, with up to 96.5% falling in spring and summer-early autumn (March to October). The meteorological data is obtained from the Fengxian meteorological station (33° 55′ N, 106° 33′ E). In ZJZ, *P. tabuliformis* is primarily distributed on southern slopes at elevations of 1400–2000 m a.s.l. (Wang et al. 2009). The soil type is forest brown soil, with a thickness of ~ 30–50 cm.

Field sampling and dendro-sample processing

For each tree, we collected four tree-ring core samples on the opposite sides of the stem (two cores for the north–south direction, two cores for the east–west direction) with a 5.15-mm-diameter increment borer (Haglöf, Långsele, Sweden). From previous tree-ring $\delta^{13}C$ analysis, four cores from different trees can guarantee the reliable values representing the site isotope chronology (Liu et al. 2012, 2015). In total, we sampled 104 tree cores from 26 mature trees, more information about tree ring growth was provided in Fig. S2. After air-drying and sanding the cores, tree rings were visually cross-dated and tree-ring width was then measured at 0.01 mm resolution using a Lintab-TSAP system (Rinntech, Heidelberg, Germany). Cross-dating was checked using the COFECHA software (Holmes 1983). Whole-ring width was detrended by fitting a cubic spline smoothing function with a 50% frequency cutoff at 67% of the series length to remove size/age-related trends and mean raw and standard chronologies were developed by using the *dplR* package in R (Bunn 2008). Ten trees were used for anatomical analyses, including four trees for stable carbon isotope ($\delta^{13}C$) measurements corresponding to those most correlated to the mean standard whole-ring width chronology. The mean longevity of these ten trees was 66 years and mean diameter was 32.3 cm. The dendro-anatomical and isotopic analysis was performed on the rings corresponding to the period from 1970 to 2017.

Dendro-anatomical analysis

The method of dendro-anatomical analysis referred to Hong et al. (2021). First, the ten cores were divided into 4–5 cm-long pieces and put in the boiling water for about 15 min to soften the wood. Then, the pieces were cut perpendicular to the axially oriented xylem with a sliding microtome (WSL-LAB-Microtome, WSL, Birmensdorf, Switzerland) (Schneider and Gärtner 2013) for obtaining flat wood surfaces. Compared with taking micro-section, the method of obtaining flat wood surfaces can avoid distortion and cell damage resulting from sectioning thin fragile samples (Liang et al. 2013). Third, the wood surfaces of pieces were stained with safranin (1% in distilled water) and these pieces were glued on a wooden sample holder. The micro surfaces were scanned using a confocal laser scanning microscope (FV1200, Olympus, Tokyo, Japan) (Liang et al. 2013) at 100 × magnification, with a resolution of 1.25 pixels μm^{-1}. The images of each year were obtained and merged using the software Adobe Photoshop CC 2019 (Adobe Systems Inc., San Jose, CA, USA). The images were then processed with WinCell Pro 2018 (Regent Instruments Inc., Québec, QC, Canada), which allowed measuring LD and CWT of all tracheids within each annual ring. Generally, 30 cell rows per ring were measured, resulting in > 7 millions of analyzed tracheids.

According to Mork's index (with a modified value of 0.83 as an efficient threshold) (Samusevich et al. 2020), the EW and LW were distinguished along the radial axis for each ring. For each core, we calculated the mean LD and mean CWT of EW and LW, respectively. To assess the climate influence on anatomical traits, the size/age-related trends were removed from these series using a similar detrending procedure as with tree-ring width data. The mean LD and CWT detrended individual series were averaged using a biweight robust mean to obtain the mean series (Fig. S3).

Stable carbon isotope analysis

Whole wood was used for $\delta^{13}C$ analyses because it shows the same iWUE trend as α-cellulose $\delta^{13}C$ (Belmecheri and Lavergne 2020). For each core, each tree ring of the 1970–2017 period was split into EW and LW parts with a dissecting scalpel under a binocular microscope. Then, the sample was put in 2 ml centrifuge tube and was milled with a ball mill (JXFSTPRP-24, Jingxin, Shanghai, China) to the fine powder. The powder samples of 70–75 μg in weight were wrapped in tin capsules and rolled into strips for stable carbon analysis. Then, the $\delta^{13}C$ of each sample was measured by an elemental analyzer (EA Isolink) linked to a mass spectrometer (Thermo Fisher Science, Bremen, Germany). The $\delta^{13}C$ was expressed with reference to the Vienna Pee Dee Belemnite (VPDB) standard and calculates as:

$$\delta^{13}\,C = \left(\frac{R_{sample}}{R_{standard}} - 1\right) \times 1000 \quad (1)$$

where R_{sample} and $R_{standard}$ are the ratios of $^{13}C/^{12}C$ of the sample and the VPDB standard, respectively. During the isotope measurement, the $\delta^{13}C$ of each sample was calibrated according to VPDB (-24.25‰ for $\delta^{13}C$). The analytical error (the standard deviation) of isotope measurements was

0.04‰ based on the repeated measurement of the standards. Suess effect caused by fossil fuel burning was removed following the procedure provided by Belmecheri and Lavergne (2020).

Calculations of iWUE

The carbon isotope discrimination ($\Delta^{13}C$) between the air carbon isotope ($\delta^{13}C_a$) and tree-ring carbon isotope ($\delta^{13}C_p$) can be expressed by Farquhar et al. (1989) as follows:

$$\triangle^{13}\,C = \frac{\delta^{13}C_a - \delta^{13}C_p}{1 + \delta^{13}C_p/1000} \quad (2)$$

The carbon isotope discrimination of C_3 plants is also related to the intercellular and atmospheric CO_2 concentration:

$$\triangle^{13}\,C = a + (b-a)(C_i/C_a) \quad (3)$$

where a (~4.4‰) represents the CO_2 discrimination caused by the CO_2 diffusion from the atmosphere into the leaf cell intercellular; b (~27‰) represents the fractionation discrimination of ribulose bisphosphate (RuBP) carboxylase against $^{13}CO_2$; C_i and C_a represent the CO_2 concentration in the intercellular spaces and the atmosphere, respectively.

The intrinsic water-use efficiency (iWUE) can be calculated by $\Delta^{13}C$, which quantifies the amount of carbon assimilated per unit of leaf area per unit of time for per unit of water cost. The iWUE is the ratio of the photosynthetic assimilation rate (A) to the stomal conductance for water vapor (g_s):

$$\text{iWUE} = \frac{A}{g_s} = \frac{C_a(1 - C_i/C_a)}{1.6} = \frac{C_a(b - \triangle^{13}C)}{1.6(b-a)} \quad (4)$$

The separated influences of CO_2 and climate on iWUE were calculated based on Voelker et al. (2016) and Liu et al. (2019). The percent change value in iWUE due to CO_2 and climate and the percent change value in iWUE due to only climate ($iWUE_{Clim}$) were first calculated and the difference between these two values was the percent change value in iWUE due to only CO_2 ($iWUE_{CO2}$). Based on the theoretical regulation of plant gas exchange in response to increasing C_a, three scenarios were considered: (i) constant C_i, (ii) constant C_i/C_a, and (iii) constant C_a—C_i (Saurer et al. 2004). These three scenarios represent different response degrees of increase in C_i to increase in C_a: (i) not at all, (ii) in a proportional way, (iii) at the same rate. More detailed explanations for these three scenarios were presented in previous studies (Saurer et al. 2004; Linares and Camarero 2011).

Climate data and statistical analysis

We used the instrumental records from the Fengxian meteorological station (33° 55′ N, 106° 33′ E, 1097 m a.s.l, 1970–2017) which is located near the sampling site. The meteorological dataset of Fengxian station was obtained from the China Meteorological Administration (http://www.cma.gov.cn/en/).

The shift years in iWUE for EW and LW were detected by *cpt.np* function in *changepoint.np* R package (Killick and Eckley 2014). Structural equation models (SEMs) were used to explore the influences of $iWUE_{CO2}$ and $iWUE_{Clim}$ and climate and their interactions on EW and LW anatomy. Firstly, we developed two initial models based on the published literature and a priori knowledge (Fig. 1). According to previous findings on *P. tabuliformis* by Hong et al. (2021), LD of EW and CWT of LW were mainly affected by spring (March–May) and summer (June–August) climate variables, respectively. In these two initial models, climate variables (i.e., precipitation and maximum temperature of spring and summer) were used to represent the early- and late-growing season climate conditions, respectively. To develop the final SEMs, we started with the initial models with initial hypothesized relationships. The initial model for EW LD hypothesized that spring temperature, precipitation and $iWUE_{CO2}$ had positive effects on EW LD while $iWUE_{Clim}$ had negative effect on EW LD (Fig. 1a). Besides, the initial model for LW CWT hypothesized that spring temperature, summer temperature and $iWUE_{Clim}$ had negative effects on LW CWT while $iWUE_{Clim}$ had negative effect on LW CWT (Fig. 1b). Secondly, a number of alternative simplified models sharing the same structure as that of initial models were built by removing non-significant ($P > 0.05$) paths one by one according to the performance of the overall model fit and the P values of the path's standard coefficient. Finally, the optimal models were selected according to model-fit statistics (goodness-of-fit index, comparative fit index, root mean square error of approximation) and by minimizing the Akaike information criterion. SEMs were performed using the *lavaan* package in R (Rosseel 2012).

Results

Trends of climate variables

EW iWUE and LW iWUE showed different years of a shift in 1989. The difference of the shift years between EW iWUE and LW iWUE maybe related to the different climatic factors affecting EW and LW. Spring temperature showed a significant increasing trend after 1989 ($P < 0.01$ for minimum, mean, and maximum temperatures; Fig. 2a), while summer temperature did not show significant increases after 1993

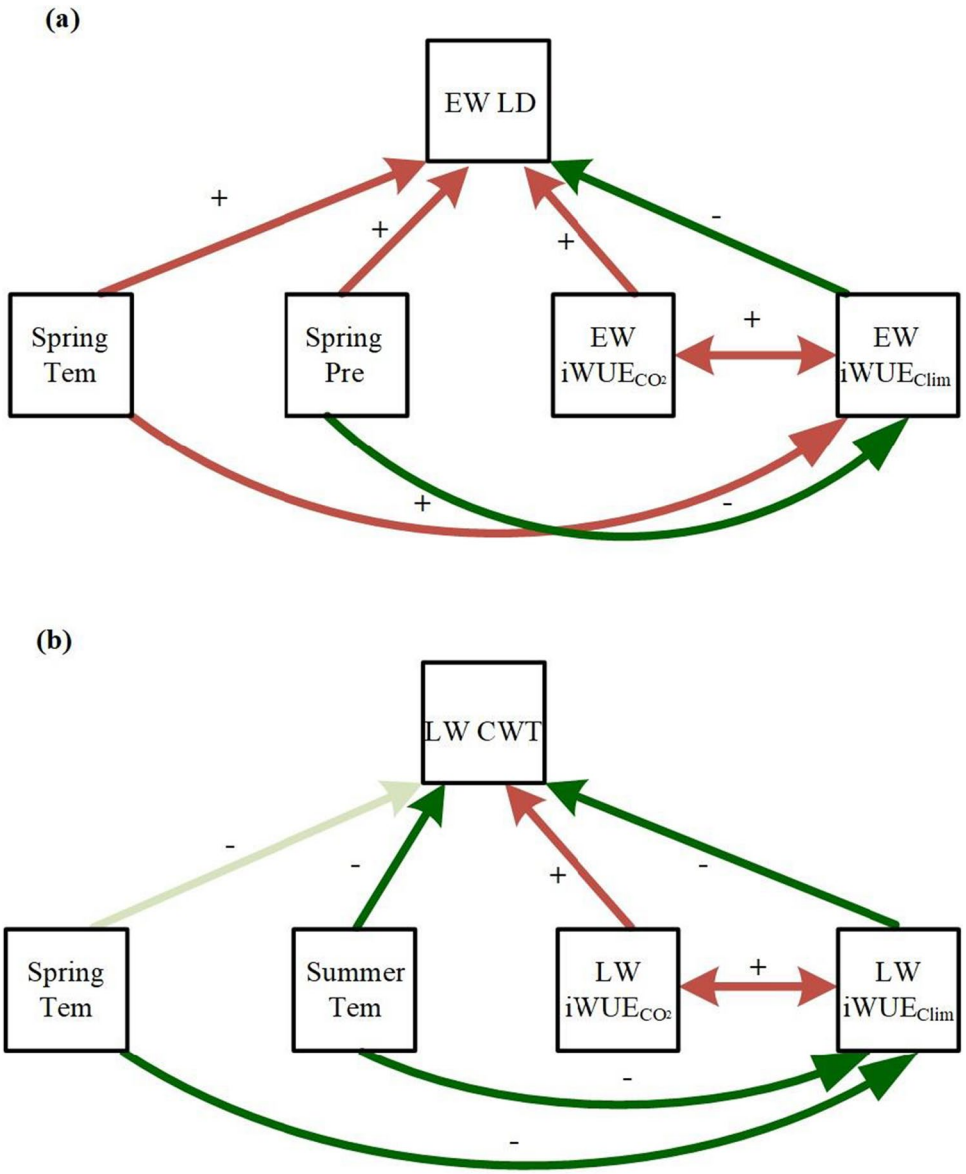

Fig. 1 The initial model shows hypothesized relationships indicating the effects of climate and intrinsic water-use efficiency [iWUE (including $iWUE_{CO2}$, $iWUE_{Clim}$)] on **a** earlywood lumen diameter (EW LD) and **b** latewood cell wall thickness (CWT). Paths with a single arrow (→) represent unidirectional relationships between variables. Paths with double-headed arrow (↔) represent correlated relationships among variables. The red paths denote positive (+) relationships, and the green paths indicate the negative (-) ones. Abbreviations: Tem, temperature; Pre, precipitation

($P > 0.05$ for minimum, mean, and maximum temperatures; Fig. 2b). There were no significant changes after the shift years (1989 for spring, 1993 for summer) for both spring ($P > 0.05$; Fig. 2a) and summer ($P > 0.05$; Fig. 2b) precipitation. For vapor pressure deficit (VPD), there was a positive and significant trend in spring ($P < 0.05$, Fig. 2a), but not in summer ($P > 0.05$; Fig. 2b). For relative humidity, spring ($P > 0.05$; Fig. 2a) and summer ($P > 0.05$; Fig. 2b) relative humidity showed decreasing trends after the shift years, but they were not significant.

Changes in iWUE and the contributions of climate and CO_2

The EW and LW iWUE values presented a significant increasing trend during 1970–1988 (slope = 0.602, $P < 0.001$) and 1970–1992 (slope = 0.413, $P < 0.05$), respectively (Fig. 3a). Compared with the former periods, the EW and LW iWUE showed steeper positive trends during 1989–2017 (slope = 1.116, $P < 0.001$) and 1993–2017 (slope = 1.263, $P < 0.001$), respectively. Thus, according to the magnitude of slopes before and after the shift years (1989 for EW iWUE, 1993 for LW iWUE), we defined the following low-iWUE periods (EW: 1970–1988, LW: 1970–1992) and high-iWUE periods (EW: 1989–2017, LW: 1993–2017), respectively. The EW iWUE and LW iWUE showed consistent high frequency variations (first-order differences) in the period 1970–1988 ($r = 0.494$, $P < 0.05$; Fig. 3b), but showed contrasting variations in the period 1989–2017 ($r = -0.283$, $P > 0.05$).

In the low-iWUE periods for EW (1970–1988) and LW (1970–1992), the changes in iWUE attributed to variation

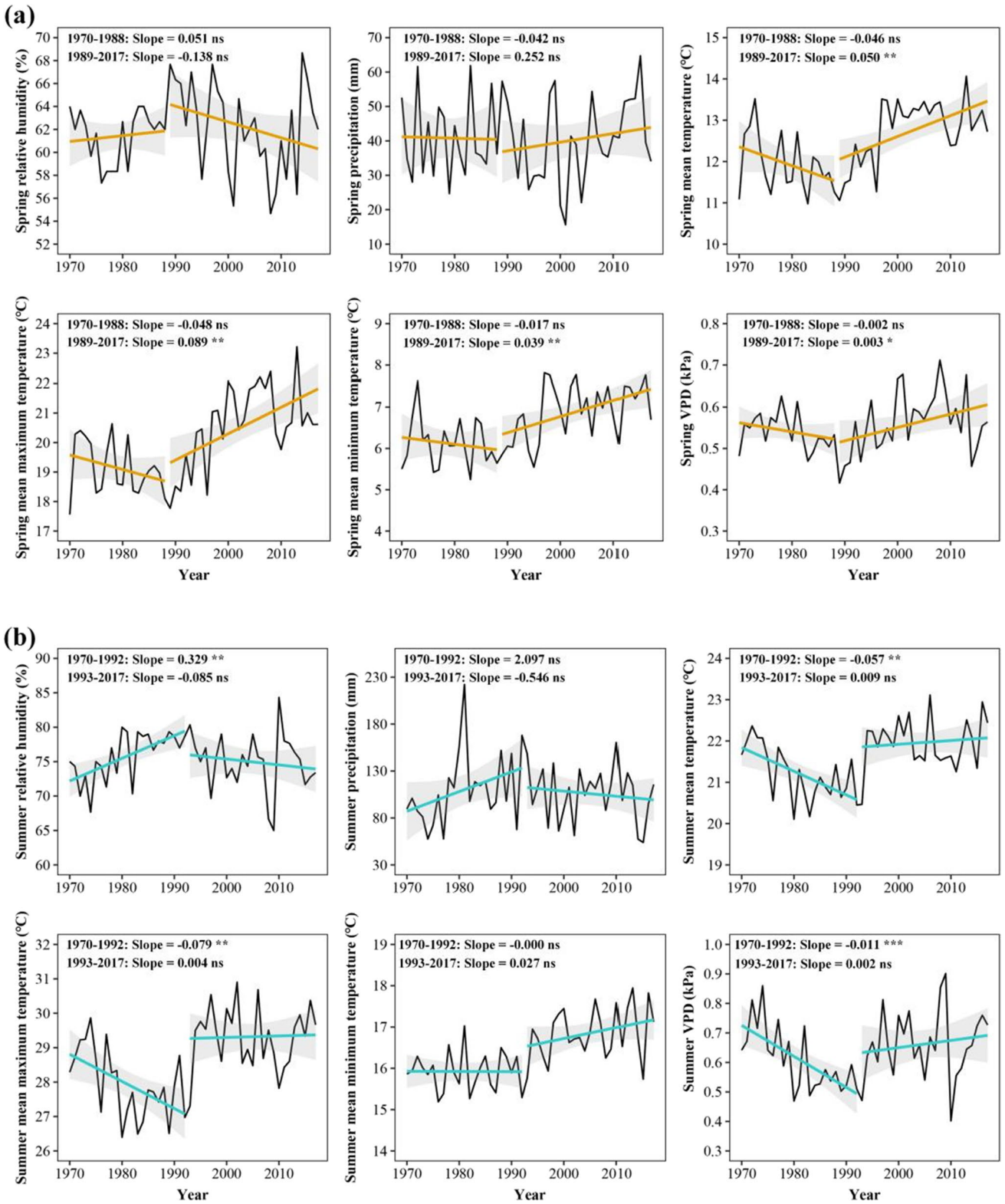

Fig. 2 Temporal variation of relative humidity, precipitation, mean temperature, mean maximum temperature, and mean minimum temperature, and vapor pressure deficit (VPD) in **a** spring (March–May) and **b** summer (June–August) during the period 1970–2017. Piecewise linear regressions were used to fit the variational trend of two subperiods (yellow lines: 1970–1988, 1989–2017; blue lines: 1970–1992 and 1993–2017). The climate values are means and the shaded areas represent standard errors of regressions. Significance levels of regressions: ns, not significant; $*P<0.05$; $**P<0.01$; $***P<0.001$

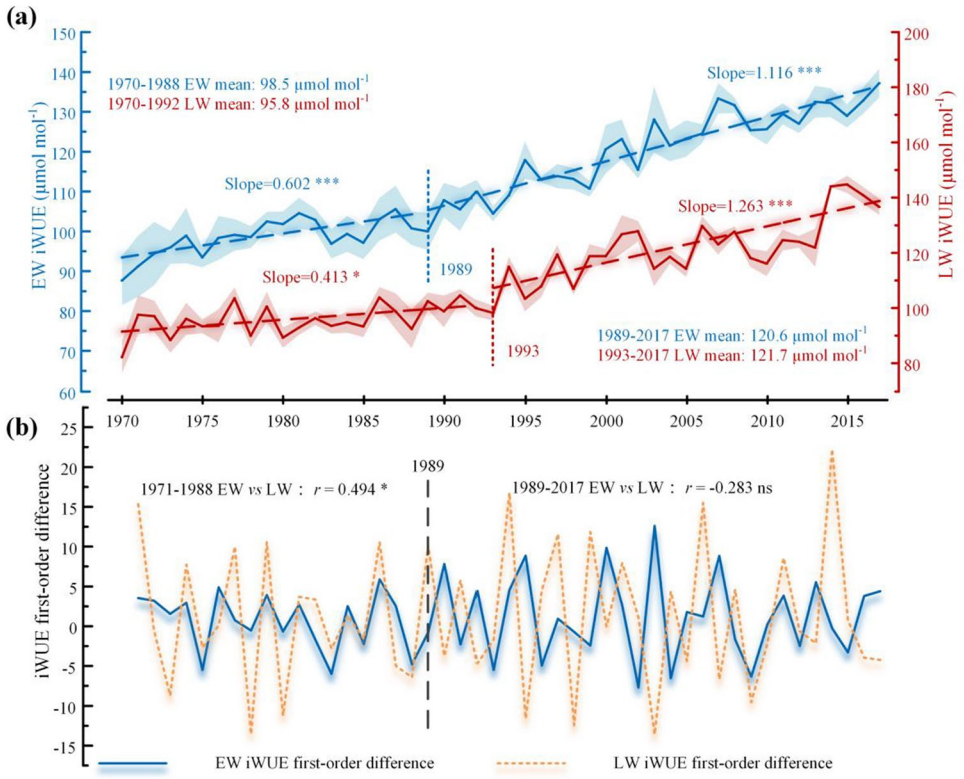

Fig. 3 **a** The temporal trends of intrinsic water-use efficiency (iWUE) for earlywood (EW) and latewood (LW) during 1970–2017. **b** The first-order differences of iWUE for EW and LW. Significance levels of regressions' slopes and correlations (*r*) between variables: ns., not significant; $*P<0.05$; $**P<0.01$; $***P<0.001$

in CO_2 and climate were positive (Fig. 4a). There was low difference between the changes in iWUE caused by the variation only by CO_2 (EW: slope = 0.311, LW: slope = 0.325) and the changes in iWUE caused by the variation only by climate (EW: slope = 0.362, LW: slope = 0.128) (Fig. 4a). Specifically, the contribution of CO_2 to iWUE was almost equal to the contribution of climate to iWUE for EW, while the contribution of CO_2 to iWUE was higher than that of climate to iWUE for LW (Fig. 4b). However, in the high-iWUE periods, the changes in iWUE attributed to variation in climate (EW: slope = 0.792, LW: slope = 0.910) were higher than those attributed to variation in CO_2 (EW: slope = 0.471, LW: slope = 0.483) (Fig. 4a). Besides, the contribution of climate to iWUE was much higher than that of CO_2 to iWUE for both EW and LW (Fig. 4b). In addition, EW iWUE (1970–1988) and LW iWUE (1970–1992) trends closely followed the predicted changes in a scenario with constant C_i/C_a (Fig. 4c). However, EW iWUE (1989–2017) and LW iWUE (1970–1992) trends followed the predicted changes in a scenario with constant C_i.

Relationships between iWUE, climate, and anatomical traits

In the low-iWUE period, spring precipitation positively affected EW LD (path coefficient: 0.50) while EW $iWUE_{CO2}$ and EW $iWUE_{Clim}$ both showed no significant influences on EW LD (Fig. 5). In contrast, spring temperature negatively affected LW CWT (path coefficient: − 0.51) while LW $iWUE_{CO2}$ and LW $iWUE_{Clim}$ both had no significant influences on LW CWT.

In the high-iWUE period, EW $iWUE_{CO2}$ had a significant positive effect (path coefficient: 0.67) but EW $iWUE_{Clim}$ had a strong negative effect (path coefficient: -0.87) on EW LD, and the total iWUE effect on EW LD was negative (path coefficient: − 0.20). Spring temperature had an indirect effect via EW $iWUE_{Clim}$ on EW LD (path coefficient: − 0.67). The total effects of iWUE (direct effects) and spring temperature (indirect effect) on EW LD was negative (total effect: − 0.86). However, LW $iWUE_{Clim}$ negatively affected LW CWT (path coefficient: − 0.62) while LW $iWUE_{CO2}$ positively affected LW CWT (path coefficient: 0.47). Ultimately, the total effect of LW iWUE was negative (path coefficient: − 0.15). Summer temperature showed an indirect effect via LW $iWUE_{Clim}$ on LW CWT (path coefficient: − 0.25). The total effects of iWUE (direct effect) and summer temperature (indirect effect) on LW CWT were negative (total effect: − 0.40).

Discussion

In this study, we quantified the direct and indirect influences of climate and iWUE on wood anatomy in low- and high-iWUE periods. We provided a new perspective to evaluate the influences of iWUE and climate on tree physiological

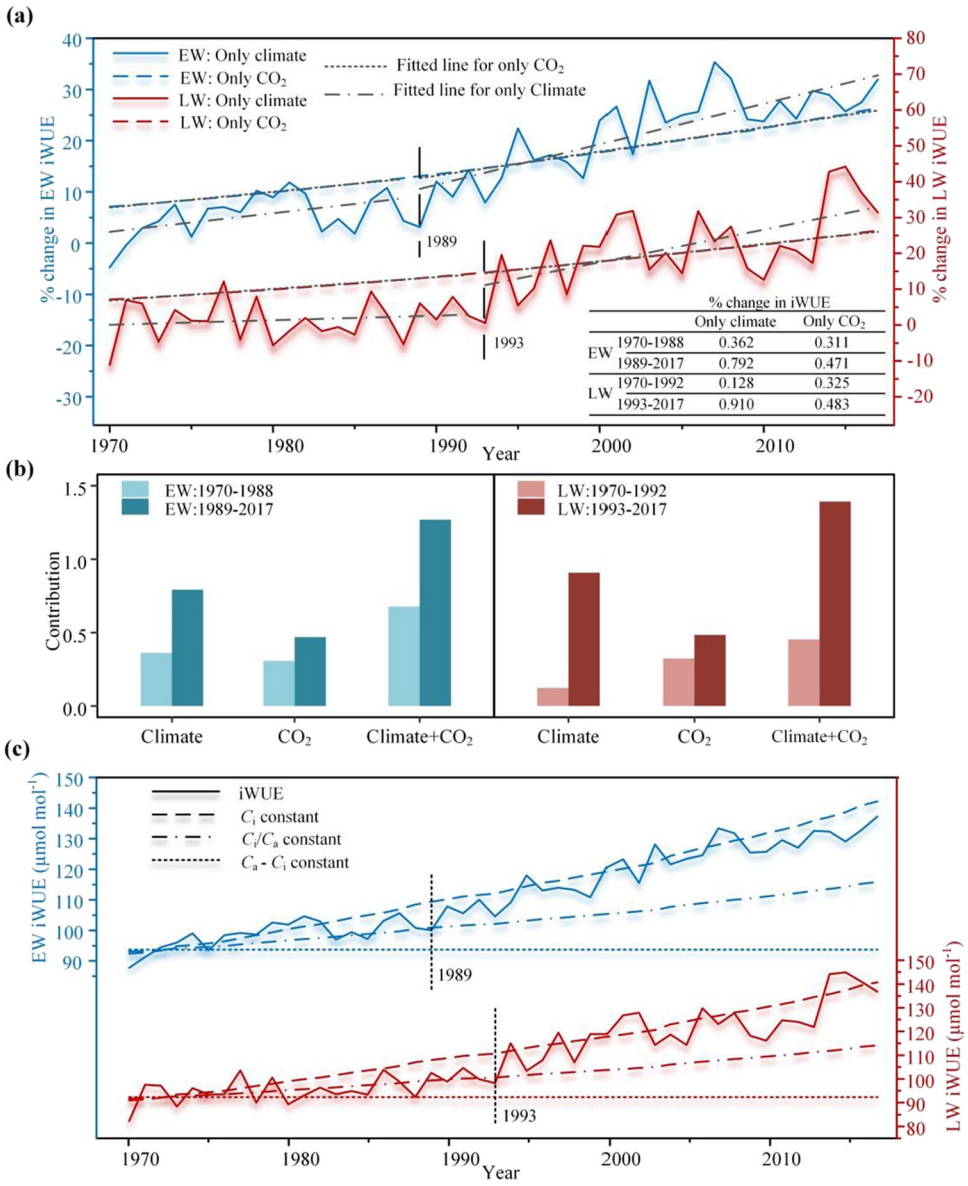

Fig. 4 **a** Percent change of intrinsic water use efficiency (iWUE) for earlywood (EW) and latewood (LW) since 1970–2017. The piece-wise linear regressions were used to fit the variational trends of iWUE caused by variation in only CO_2 (dotted line) or only climate (dash-and-dot line). The values in the inset table showed the slope of liner regressions in different periods (EW: 1970–1988 and 1989–2017; LW: 1970–1992 and 1993–2017). **b** The estimation of the contribution of only climate, only CO_2, and climate + CO_2 to changes in iWUE for EW and LW in different periods. **c** The temporal change of estimated iWUE was based on tree-ring $\delta^{13}C$. Based on the theoretical regulation of plant gas exchange in response to increasing atmospheric CO_2 (C_a), three models were considered: constant intercellular CO_2 (C_i), constant C_i/C_a, and constant C_a-C_i (Saurer et al. 2004). The iWUE was held constant in the first 5-year mean values for EW and LW, respectively. The atmospheric CO_2 concentration and $\delta^{13}C$ were obtained from Belmecheri and Lavergne (2020)

processes that are closely related to tree growth, potential hydraulic functions, and carbon allocation from a high-resolution scale (cellular scale) by taking into account the potential indirect effects of climate via iWUE on these physiological processes.

In the low-iWUE period (1970 to ~ 1989) with a relatively cool climate, wood anatomical traits of *P. tabuliformis* were affected by spring precipitation and temperature without relevant impacts of CO_2 fertilization (Fig. 5). Specifically, spring precipitation had a direct and positive influence on cell enlargement of EW, which was supported by previous studies (Zhang et al. 2018; Hong et al. 2021). Favorable spring water status leads to positive turgor pressure and thus promoted cell enlargement in the early growing season (Hsiao 1973). This finding was also consistent with previous studies showing a positive water balance during the early growing season not only promoted cell enlargement and tree growth but also improved hydraulic conductivity (Wagner et al. 2012; Pacheco et al. 2016; Castagneri et al. 2017; Huang et al. 2020; Hong et al. 2021). However, high spring temperatures had a negative effect on LW cell-wall thickening, indicating less carbon fixation in LW formation (Hong et al. 2021). During the low-iWUE period, the climate was relatively wet and cool (Fig. 2), which was beneficial for EW tracheid radial enlargement and LW cell-wall thickening. In addition, although the contribution of CO_2 to iWUE was dominant during the low-iWUE periods of EW and LW (Fig. 4b), the impact of iWUE on wood anatomy was not significant, probably as a result of the relatively low CO_2 concentration caused relatively low iWUE.

In the high-iWUE period (~ 1989–2017) with a relatively warm climate, considering the strong influences of climate

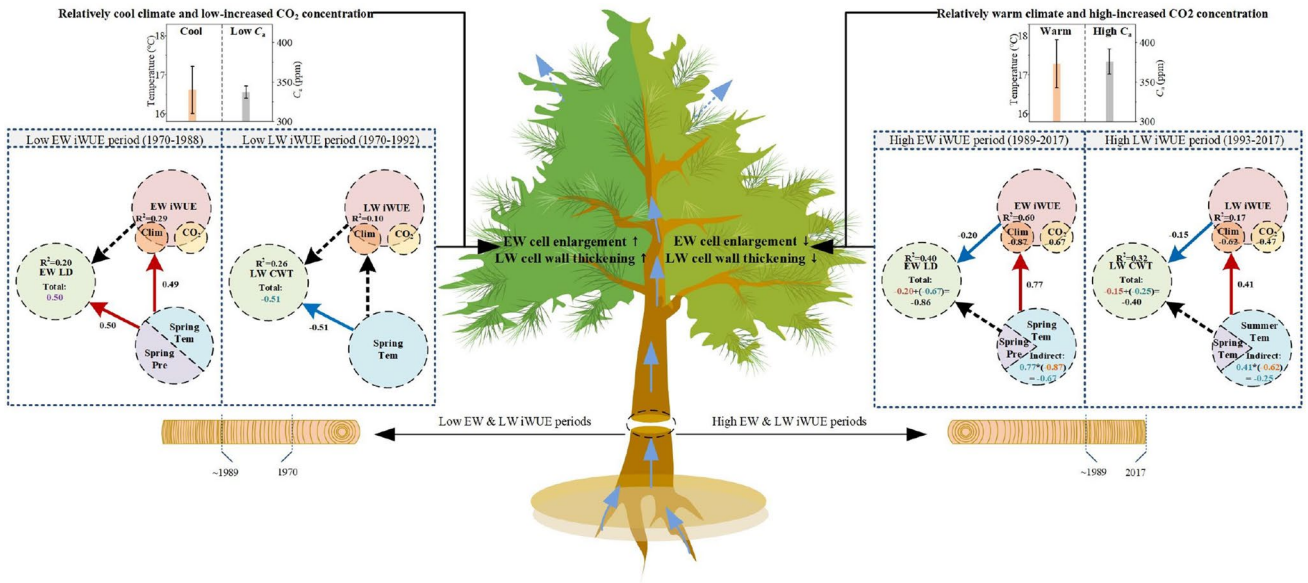

Fig. 5 Diagram showing the postulated effects of climate and intrinsic water-use efficiency (iWUE) on tree-ring wood anatomy [earlywood lumen diameter (EW LD) and latewood cell wall thickness (LW CWT)] for two subperiods with low and high iWUE, respectively. EW: 1970–1988 with low iWUE, 1989–2017 with high iWUE; LW: 1970–1992 with low iWUE, 1993–2017 with high iWUE. The schematic diagram below was constructed according to the results of structural equation models (SEMs) (Figs. S4 and S5). The lines with a single arrow (→) represent unidirectional relationships between variables. Except for path linkages between iWUE and wood anatomy parameters, the coefficient of each line is the standardized path coefficient in SEMs. Two small circles at the bottom of iWUE are $iWUE_{Clim}$ (abbreviated as Clim) and $iWUE_{CO2}$ (abbreviated as CO_2). The coefficients in these two circles show their separate effects on wood anatomy, respectively. Thus, the coefficient of lines from iWUE to anatomical parameters represents the sum effects of $iWUE_{CO2}$ and $iWUE_{Clim}$ on anatomical parameters. The indirect effects of climate on wood anatomy are shown in blue circles. The total effects of climates and (or) iWUE are shown in green circles. The black dashed lines represent non-significant effects ($P > 0.05$). The red and blue solid lines represent significant ($P < 0.05$) positive and negative effects, respectively

on iWUE changes, the responses of EW LD and LW CWT to iWUE, climate, and their interaction became more complex than those observed during the low-iWUE period (Fig. 5). In this period, CO_2 showed positive links with EW cell enlargement and LW cell-wall thickening, which promoted tree growth and structural carbon fixation in cell walls. Previous study conducted in northern Patagonia found that a reduction in iWUE caused by increased carbon assimilation related to increasing CO_2 atmospheric to an extent coupled with thicker cell walls, which suggested that the coupling response of water use-efficiency and wood anatomy to climate variations (Puchi et al. 2021). In this study, the increase in CO_2 by stimulating photosynthesis is not only essential for the synthesis of cell-wall products, but also for maintaining the expansion pressure of cell turgor, which has been supported by previous studies (Atkinson and Taylor 1996; Kostiainen et al. 2014; Kim et al. 2015). However, spring and summer showed warming trends, especially for spring since ~ 1989 (Fig. 2), and a warming climate accompanied with enhanced transpiration demand would exacerbate drought stress. High EW and LW $iWUE_{Clim}$, attributed to warming and drying climate conditions (Fig. 2), had stronger constraining effects on EW cell enlargement and LW cell-wall deposition than any fertilization effect due to rising CO_2. Previous studies also reported that improved iWUE could not compensate for tree growth decline triggered by drought stress (Linares and Camarero 2011; Levesque et al. 2014; Frank et al. 2015; Urrutia-Jalabert et al. 2015; Fernández-de-Uña et al. 2016; Xu et al. 2018; Liu et al. 2019; Marchand et al. 2020; Heilman et al. 2021). The possibility of this phenomenon was related to the photosynthetic pathway of species (C_3 and C_4), the threshold of CO_2 concentration and temperature tipping point of photosynthesis (Reich et al. 2018; Rahman et al. 2019; Duffy et al. 2021). Specifically, C_4 species are less in response to elevated CO_2 than C_3 species, and this pattern would reverse with the extension of experimental time. Photosynthetic efficiency would no longer rise or even decrease when the CO_2 concentration reaches a certain level. In addition, plant photosynthesis of leave increases with the temperature up to an optimum temperature while above the optimum temperature, foliar photosynthesis sharply decreases (Huang et al. 2019). Therefore, due to the increase in temperature and possibly exceeding the optimal foliar photosynthetic temperature in the high-iWUE period, A possibly reduce on the one hand, and the g_s may further reduce on the other hand, showing that high iWUE could not compensate for the decline in tree growth caused by drought.

During the high-iWUE period, probably caused by the decline of g_s, there was a reduction of EW LD and LW CWT. The scenario of constant C_i indicates the strong regulation of g_s or the enhancement of A while the scenario of constant C_i/C_a reflects proportional regulation of A and g_s (Saurer et al. 2004). In our study, iWUE was consistent with constant C_i/C_a scenarios during low-iWUE periods, while iWUE was consistent with constant C_i scenarios (the scenario that predicted the strongest response to increasing C_a) in response to increasing CO_2 during high-iWUE periods (Fig. 4c). In addition, we found that EW C_i and LW C_i almost remained stable, while EW C_i/C_a and LW C_i/C_a decreased during the high-iWUE period (Fig. S6). This indicated that the constraint of g_s became stronger or A increased and thus resulted in the increasing EW and LW iWUE in the high-iWUE period (Saurer et al. 2004; Liu et al. 2014; Urrutia-Jalabert et al. 2015). However, A may not increase too much or even remained relatively stable during ~ 1990–2017 because a reduced growth was observed during this period (Fig. S7). This suggests indirectly that decreased g_s may contribute to increasing iWUE more than increased A for both EW and LW during the high-iWUE period. Thus, we considered that the decline of g_s played a major role in the increasing EW and LW iWUE during the high-iWUE period, and therefore, g_s was deeply affected by drought stress. Thus, spring drought stress probably induced stomata closure, the decline of g_s and the increase of EW $iWUE_{Clim}$ (Fig. 4a). This may be further associated with the formation of EW tracheids with smaller lumen. It is widely known that the xylem structural characteristics are closely related to the hydraulic function of trees. Hong et al. (2021) found that EW lumen size (LD) was the main anatomy-related contributor influencing conduit wall reinforcement, a surrogate of xylem embolism resistance (Hacke et al. 2015). Moreover, plants with smaller conduits usually show lower hydraulic conductivity, but are less prone to drought-induced embolism and have better performance under higher xylem tension (Gleason et al. 2016; Epila et al. 2017). Thus, the smaller LD of EW would increase the hydraulic safety of *P. tabuliformis* at the expense of growth in the early growing season. For LW, a decrease in g_s contributed to the increase of LW $iWUE_{Clim}$ under warm summer conditions (Fig. 4a), which further resulted in lower carbon uptake and the formation of thin cell-wall tracheids with a lower carbon cost in the late growing season.

The present study allowed us to speculate on future xylem anatomy of *P. tabuliformis* in response to increasing CO_2 concentration and climate warming. According to the two mechanisms of plant mortality (i.e., hydraulic failure and carbon starvation), a reduction in stomatal conductance rate can minimize water loss and hydraulic failure during drought, thereby reducing the carbon uptake rate (Tyree and Zimmermann 2002; McDowell et al. 2008; Sevanto et al. 2014). The direct $iWUE_{Clim}$ and indirect climate negative effects on EW LD were stronger than those found on LW CWT (Fig. 5), indicating the improvement of potential hydraulic safety in the early growing season but a shift towards a decline in structural carbon fixation in the late growing season. Thus, we considered that future warmer and dryer climate conditions will probably lead to the enhancement of potential hydraulic safety in the early growing season and cause a decline in carbon uptake and fixation during the late growing season.

In conclusion, spring climate exhibited significant and dominant effects on EW cell enlargement and LW cell wall deposition during the low-iWUE periods. Relatively wet and cool climate conditions promoted cell enlargement and wall thickening before ~ 1989. However, the effects of rising C_a and warming climate and their interaction on EW and LW anatomical traits became complex afterward. Increased $iWUE_{CO2}$ could not compensate for the decline of cell enlargement in EW and carbon storage in LW cell walls related to climate. Moreover, the negative direct effects of $iWUE_{Clim}$ and the indirect effects of climate on EW LD were stronger than those acting on LW CWT. This suggests that *P. tabuliformis* will face a potential risk of growth and carbon uptake decline, but the formation of narrow conduits will decrease the potential risk of drought-induced xylem embolism.

In our study, wood rather than α-cellulose was used for $\delta^{13}C$ analysis. Trends in $\delta^{13}C$ are little different between obtained from wood and obtained from α-cellulose. Besides, the trend of $\delta^{13}C$ as well as iWUE obtained from wood is same with that of obtained from α-cellulose, which has been confirmed by many previous studies for multiple species.

Although we have identified the varied contribution of rising C_a and warming climate to xylem anatomical traits, more works need along similar climate gradients to provide a holistic understanding of temperate forests in response to rapid climate change. The mixed responses of trees to elevated C_a and warming climate should be considered into ecological models for more accurate forecasts of temperate forest dynamics in a warming future.

Supplementary Information The online version contains supplementary material available at https://doi.org/10.1007/s00484-023-02475-7.

Funding Xiaohong Liu was supported by the National Natural Science Foundation of China (Grant 41971104) and Fundamental Research Funds for the Central Universities (Project GK202206032). Yixue Hong and Yu Zhang funded by Fundamental Research Funds for the Central Universities (Projects 2020CSLY011, 2020CBLY010).

Declarations

Conflict of interest The authors declare no competing interests.

References

Allen CD, Breshears DD, McDowell NG (2015) On underestimation of global vulnerability to tree mortality and forest die-off from hotter drought in the Anthropocene. Ecosphere 6(8):1–55. https://doi.org/10.1890/es15-00203.1

Andreu-Hayles L, Planells O, GutiÉRrez E, Muntan E, Helle G, Anchukaitis KJ, Schleser GH (2011) Long tree-ring chronologies reveal 20th century increases in water-use efficiency but no enhancement of tree growth at five Iberian pine forests. Glob Change Biol 17(6):2095–2112. https://doi.org/10.1111/j.1365-2486.2010.02373.x

Atkinson CJ, Taylor JM (1996) Effects of elevated CO2 on stem growth, vessel area and hydraulic conductivity of oak and cherry seedlings. New Phytol 133(4):617–626. https://doi.org/10.1111/j.1469-8137.1996.tb01930.x

Battipaglia G, Saurer M, Cherubini P, Calfapietra C, McCarthy HR, Norby RJ, Francesca CM (2013) Elevated CO_2 increases tree-level intrinsic water use efficiency: insights from carbon and oxygen isotope analyses in tree rings across three forest FACE sites. New Phytol 197(2):544–554. https://doi.org/10.1111/nph.12044

Belmecheri S, Lavergne A (2020) Compiled records of atmospheric CO_2 concentrations and stable carbon isotopes to reconstruct climate and derive plant ecophysiological indices from tree rings. Dendrochronologia. 63:125748. https://doi.org/10.1016/j.dendro.2020.125748

Belmecheri S, Maxwell RS, Taylor AH, Davis KJ, Guerrieri R, Moore DJP, Rayback SA (2021) Precipitation alters the CO_2 effect on water-use efficiency of temperate forests. Glob Change Biol 27(8):1560–1571. https://doi.org/10.1111/gcb.15491

Brito P, Grams TE, Matysssek R, Jimenez MS, Gonzalez-Rodriguez AM, Oberhuber W, Wieser G (2016) Increased water use efficiency does not prevent growth decline of *Pinus canariensis* in a semi-arid treeline ecotone in Tenerife, Canary Islands (Spain). Ann for Sci 73(3):741–749. https://doi.org/10.1007/s13595-016-0562-5

Bunn AG (2008) A dendrochronology program library in R (dplR). Dendrochronologia 26(2):115–124. https://doi.org/10.1016/j.dendro.2008.01.002

Camarero JJ, Gazol A, Galvan JD, Sanguesa-Barreda G, Gutierrez E (2015) Disparate effects of global-change drivers on mountain conifer forests: warming-induced growth enhancement in young trees vs. CO2 fertilization in old trees from wet sites. Glob Change Biol 21(2):738–749. https://doi.org/10.1111/gcb.12787

Castagneri D, Fonti P, von Arx G, Carrer M (2017) How does climate influence xylem morphogenesis over the growing season? Insights from long-term intra-ring anatomy in *Picea abies*. Ann Bot 119(6):1011–1020. https://doi.org/10.1093/aob/mcw274

Castagneri D, Prendin AL, Peters RL, Carrer M, von Arx G, Fonti P (2020) Long-term impacts of defoliator outbreaks on Larch xylem structure and tree-ring biomass. Front Plant Sci 11:1078. https://doi.org/10.3389/fpls.2020.01078

Cuny HE, Rathgeber CB, Frank D, Fonti P, Makinen H, Prislan P, Rossi S, Del Castillo EM, Campelo F, Vavrcik H, Camarero JJ, Bryukhanova MV, Jyske T, Gricar J, Gryc V, De Luis M, Vieira J, Cufar K, Kirdyanov AV, Oberhuber W, Treml V, Huang JG, Li X, Swidrak I, Deslauriers A, Liang E, Nojd P, Gruber A, Nabais C, Morin H, Krause C, King G, Fournier M (2015) Woody biomass production lags stem-girth increase by over one month in coniferous forests. Nat Plants 1:15160. https://doi.org/10.1038/nplants.2015.160

Drake JE, Aspinwall MJ, Pfautsch S, Rymer PD, Reich PB, Smith RA, Crous KY, Tissue DT, Ghannoum O, Tjoelker MG (2015) The capacity to cope with climate warming declines from temperate to tropical latitudes in two widely distributed Eucalyptus species. Glob Change Biol 21(1):459–472. https://doi.org/10.1111/gcb.12729

Duffy KA, Schwalm CR, Arcus VL, Koch GW, Liang LL, Schipper LA (2021) How close are we to the temperature tipping point of the terrestrial biosphere? Sci Adv 7(3):eaay1052. https://doi.org/10.1126/sciadv.aay1052

Eilmann B, Zweifel R, Buchmann N, Fonti P, Rigling A (2009) Drought-induced adaptation of the xylem in Scots pine and pubescent oak. Tree Physiol 29(8):1011–1020. https://doi.org/10.1093/treephys/tpp035

Epila J, De Baerdemaeker NJF, Vergeynst LL, Maes WH, Beeckman H, Steppe K (2017) Capacitive water release and internal leaf water relocation delay drought-induced cavitation in African Maesopsis eminii. Tree Physiol 37(4):481–490. https://doi.org/10.1093/treephys/tpw128

Farquhar GD, Ehleringer JR, Hubick KT (1989) Carbon siotope discrimination and photosynthesis. Annu Rev Plant Physiol Plant Mol Biol 40:503–537. https://doi.org/10.1146/annurev.pp.40.060189.002443

Fernández-de-Uña L, McDowell NG, Cañellas I, Gea-Izquierdo G, Canham C (2016) Disentangling the effect of competition, CO2and climate on intrinsic water-use efficiency and tree growth. J Ecol 104(3):678–690. https://doi.org/10.1111/1365-2745.12544

Fonti P, Babushkina EA (2016) Tracheid anatomical responses to climate in a forest-steppe in Southern Siberia. Dendrochronologia 39:32–41. https://doi.org/10.1016/j.dendro.2015.09.002

Fonti P, von Arx G, Garcia-Gonzalez I, Eilmann B, Sass-Klaassen U, Gartner H, Eckstein D (2010) Studying global change through investigation of the plastic responses of xylem anatomy in tree rings. New Phytol 185(1):42–53. https://doi.org/10.1111/j.1469-8137.2009.03030.x

Frank DC, Poulter B, Saurer M, Esper J, Huntingford C, Helle G, Treydte K, Zimmermann NE, Schleser GH, Ahlström A, Ciais P, Friedlingstein P, Levis S, Lomas M, Sitch S, Viovy N, Andreu-Hayles L, Bednarz Z, Berninger F, Boettger T, D'Alessandro CM, Daux V, Filot M, Grabner M, Gutierrez E, Haupt M, Hilasvuori E, Jungner H, Kalela-Brundin M, Krapiec M, Leuenberger M, Loader NJ, Marah H, Masson-Delmotte V, Pazdur A, Pawelczyk S, Pierre M, Planells O, Pukiene R, Reynolds-Henne CE, Rinne KT, Saracino A, Sonninen E, Stievenard M, Switsur VR, Szczepanek M, Szychowska-Krapiec E, Todaro L, Waterhouse JS, Weigl M (2015) Water-use efficiency and transpiration across European forests during the Anthropocene. Nat Clim Chang 5(6):579–583. https://doi.org/10.1038/nclimate2614

Fritts HC (1976) Tree Rings and Climate, 1st edn. Academic Press, London. https://doi.org/10.1016/B978-0-12-268450-0.X5001-0

Gagen M, Finsinger W, Wagner-Cremer F, McCarroll D, Loader NJ, Robertson I, Jalkanen R, Young G, Kirchhefer A (2011) Evidence of changing intrinsic water-use efficiency under rising atmospheric CO_2 concentrations in Boreal Fennoscandia from subfossil leaves and tree ring $\delta^{13}C$ ratios. Glob Change Biol 17(2):1064–1072. https://doi.org/10.1111/j.1365-2486.2010.02273.x

Gao T, Yin S, Wang S (2018) Spatial and temporal variations of drought in northern and southern regions of Qinling Mountains based on standardized precipitation evapotranspiration index. Arid Land Geogr 41(4):761–770

Giguere-Croteau C, Boucher E, Bergeron Y, Girardin MP, Drobyshev I, Silva LCR, Helie JF, Garneau M (2019) North America's oldest boreal trees are more efficient water users due to increased [CO_2], but do not grow faster. Proc Natl Acad Sci USA 116(7):2749–2754. https://doi.org/10.1073/pnas.1816686116

Gleason SM, Westoby M, Jansen S, Choat B, Hacke UG, Pratt RB, Bhaskar R, Brodribb TJ, Bucci SJ, Cao KF, Cochard H, Delzon S, Domec JC, Fan ZX, Feild TS, Jacobsen AL, Johnson DM, Lens F, Maherali H, Martinez-Vilalta J, Mayr S, McCulloh KA, Mencuccini M, Mitchell PJ, Morris H, Nardini A, Pittermann J,

Plavcova L, Schreiber SG, Sperry JS, Wright IJ, Zanne AE (2016) Weak tradeoff between xylem safety and xylem-specific hydraulic efficiency across the world's woody plant species. New Phytol 209(1):123–136. https://doi.org/10.1111/nph.13646

González Muñoz N, Linares JC, Castro-Díez P and Sass-Klaassen U (2015) Contrasting secondary growth and water use efficiency patterns in native and exotic trees co-occurring in inner Spain riparian forests. For Syst 24(1). https://doi.org/10.5424/fs/20152441-06586

Hacke UG, Lachenbruch B, Pittermann J, Mayr S, Domec JC, Schulte PJ (2015) The hydraulic architecture of conifers. In: Hacke UG (ed) Functional and Ecological Xylem, Anatomy. Springer Cham, Switzerland, pp 39–75

Heilman KA, Trouet VM, Belmecheri S, Pederson N, Berke MA, McLachlan JS (2021) Increased water use efficiency leads to decreased precipitation sensitivity of tree growth, but is offset by high temperatures. Oecologia 197(4):1095–1110. https://doi.org/10.1007/s00442-021-04892-0

Holmes RL (1983) Computer-assisted quality control in tree-ring dating and measurement. Tree-Ring Bullet 43:69–78

Hong Y, Zhang L, Liu X, Aritsara ANA, Zeng X, Xing X, Lu Q, Wang K, Wang Y, Zhang Y, Wang W (2021) Tree ring anatomy indices of Pinus tabuliformis revealed the shifted dominant climate factor influencing potential hydraulic function in western Qinling Mountains. Dendrochronologia 70:125881. https://doi.org/10.1016/j.dendro.2021.125881

Hsiao TC (1973) Plant responses to water stress. Ann Rev Plant Physiol 24:519–570. https://doi.org/10.1146/annurev.pp.24.060173.002511

Huang JG, Bergeron Y, Denneler B, Berninger F, Tardif J (2007) Response of forest trees to increased atmospheric CO_2. Crit Rev Plant Sci 26(5–6):265–283. https://doi.org/10.1080/07352680701626978

Huang M, Piao S, Ciais P, Penuelas J, Wang X, Keenan TF, Peng S, Berry JA, Wang K, Mao J, Alkama R, Cescatti A, Cuntz M, De Deurwaerder H, Gao M, He Y, Liu Y, Luo Y, Myneni RB, Niu S, Shi X, Yuan W, Verbeeck H, Wang T, Wu J, Janssens IA (2019) Air temperature optima of vegetation productivity across global biomes. Nat Ecol Evol 3(5):772–779. https://doi.org/10.1038/s41559-019-0838-x

Huang JG, Ma Q, Rossi S, Biondi F, Deslauriers A, Fonti P, Liang E, Makinen H, Oberhuber W, Rathgeber CBK, Tognetti R, Treml V, Yang B, Zhang JL, Antonucci S, Bergeron Y, Camarero JJ, Campelo F, Cufar K, Cuny HE, De Luis M, Giovannelli A, Gricar J, Gruber A, Gryc V, Guney A, Guo X, Huang W, Jyske T, Kaspar J, King G, Krause C, Lemay A, Liu F, Lombardi F, Martinez Del Castillo E, Morin H, Nabais C, Nojd P, Peters RL, Prislan P, Saracino A, Swidrak I, Vavrcik H, Vieira J, Yu B, Zhang S, Zeng Q, Zhang Y, Ziaco E (2020) Photoperiod and temperature as dominant environmental drivers triggering secondary growth resumption in Northern Hemisphere conifers. Proc Natl Acad Sci USA 117(34):20645–20652. https://doi.org/10.1073/pnas.2007058117

Joos F, Spahni R (2008) Rates of change in natural and anthropogenic radiative forcing over the past 20,000 years. Proc Natl Acad Sci USA 105(5):1425–1430. https://doi.org/10.1073/pnas.0707386105

Kannenberg SA, Driscoll AW, Szejner P, Anderegg WRL, Ehleringer JR (2021) Rapid increases in shrubland and forest intrinsic water-use efficiency during an ongoing megadrought. Proc Natl Acad Sci USA. 118(52):e1118052118. https://doi.org/10.1073/pnas.2118052118

Killick R, Eckley I (2014) changepoint: an R package for changepoint analysis. J Stat Softw. 58(3):1–19. https://doi.org/10.18637/jss.v058.i03

Kim K, Labbe N, Warren JM, Elder T, Rials TG (2015) Chemical and anatomical changes in Liquidambar styraciflua L. xylem after long term exposure to elevated CO2. Environ Pollut 198:179–85. https://doi.org/10.1016/j.envpol.2015.01.006

Kostiainen K, Saranpaa P, Lundqvist SO, Kubiske ME, Vapaavuori E (2014) Wood properties of Populus and Betula in long-term exposure to elevated CO(2) and O(3). Plant Cell Environ 37(6):1452–1463. https://doi.org/10.1111/pce.12261

Levesque M, Siegwolf R, Saurer M, Eilmann B, Rigling A (2014) Increased water-use efficiency does not lead to enhanced tree growth under xeric and mesic conditions. New Phytol 203(1):94–109. https://doi.org/10.1111/nph.12772

Li D, Fang K, Li Y, Chen D, Liu X, Dong Z, Zhou F, Guo G, Shi F, Xu C, Li Y (2017) Climate, intrinsic water-use efficiency and tree growth over the past 150 years in humid subtropical China. PLoS One 12(2):e0172045. https://doi.org/10.1371/journal.pone.0172045

Li Y, Dong Z, Chen D, Zhao S, Zhou F, Cao X, Fang K (2019) Growth decline of *Pinus Massoniana* in response to warming induced drought and increasing intrinsic water use efficiency in humid subtropical China. Dendrochronologia 57:125609. https://doi.org/10.1016/j.dendro.2019.125609

Liang W, Heinrich I, Helle G, Liñán ID, Heinken T (2013) Applying CLSM to increment core surfaces for histometric analyses: a novel advance in quantitative wood anatomy. Dendrochronologia 31(2):140–145. https://doi.org/10.1016/j.dendro.2012.09.002

Linares JC, Camarero JJ (2011) Growth patterns and sensitivity to climate predict silver fir decline in the Spanish Pyrenees. Eur J for Res 131(4):1001–1012. https://doi.org/10.1007/s10342-011-0572-7

Liu Y, Wang R, Leavitt SW, Song H, Linderholm HW, Li Q, An Z (2012) Individual and pooled tree-ring stable-carbon isotope series in Chinese pine from the Nan Wutai region, China: common signal and climate relationships. Chem Geol. 330–331:17–26. https://doi.org/10.1016/j.chemgeo.2012.08.008

Liu H, Park Williams A, Allen CD, Guo D, Wu X, Anenkhonov OA, Liang E, Sandanov DV, Yin Y, Qi Z, Badmaeva NK (2013a) Rapid warming accelerates tree growth decline in semi-arid forests of Inner Asia. Glob Change Biol 19(8):2500–2510. https://doi.org/10.1111/gcb.12217

Liu N, Liu Y, Zhou Q, Bao G (2013b) Droughts and broad-scale climate variability reflected by temperature-sensitive tree growth in the Qinling Mountains, central China. Int J Biometeorol 57(1):169–177. https://doi.org/10.1007/s00484-012-0544-8

Liu X, Wang W, Xu G, Zeng X, Wu G, Zhang X, Qin D (2014) Tree growth and intrinsic water-use efficiency of inland riparian forests in northwestern China: evaluation via $\delta^{13}C$ and $\delta^{18}O$ analysis of tree rings. Tree Physiol 34(9):966–980. https://doi.org/10.1093/treephys/tpu067

Liu X, An W, Treydte K, Wang W, Xu G, Zeng X, Wu G, Wang B, Zhang X (2015) Pooled versus separate tree-ring deltaD measurements, and implications for reconstruction of the Arctic Oscillation in northwestern China. Sci Total Environ 511:584–94. https://doi.org/10.1016/j.scitotenv.2015.01.002

Liu B, Liang E, Liu K, Camarero J (2018) Species- and elevation-dependent growth responses to climate warming of mountain forests in the Qinling Mountains, central China. Forests 9(5):248. https://doi.org/10.3390/f9050248

Liu X, Zhao L, Voelker S, Xu G, Zeng X, Zhang X, Zhang L, Sun W, Zhang Q, Wu G, Li X (2019) Warming and CO_2 enrichment modified the ecophysiological responses of Dahurian larch and Mongolia pine during the past century in the permafrost of northeastern China. Tree Physiol 39(1):88–103. https://doi.org/10.1093/treephys/tpy060

Lu W, Yu X, Jia G, Li H, Liu Z (2018) Responses of intrinsic water-use efficiency and tree growth to climate change in semi-arid areas of north China. Sci Rep 8(1):308. https://doi.org/10.1038/s41598-017-18694-z

Ma X, Bai H, Deng C, Wu T (2019) Sensitivity of vegetation on alpine and subalpine timberline in Qinling mountains to temperature change. Forests 10(12):1105. https://doi.org/10.3390/f10121105

Marchand W, Girardin MP, Hartmann H, Depardieu C, Isabel N, Gauthier S, Boucher E, Bergeron Y (2020) Strong overestimation of water-use efficiency responses to rising CO_2 in tree-ring studies. Glob Chang Biol 26(8):4538–4558. https://doi.org/10.1111/gcb.15166

McCarroll D, Loader NJ (2004) Stable isotopes in tree rings. Quat Sci Rev 23(7–8):771–801. https://doi.org/10.1016/j.quascirev.2003.06.017

McDowell N, Pockman WT, Allen CD, Breshears DD, Cobb N, Kolb T, Plaut J, Sperry J, West A, Williams DG, Yepez EA (2008) Mechanisms of plant survival and mortality during drought: why do some plants survive while others succumb to drought? New Phytol 178(4):719–739. https://doi.org/10.1111/j.1469-8137.2008.02436.x

Nock CA, Baker PJ, Wanek W, Leis A, Grabner M, Bunyavejchewin S, Hietz P (2011) Long-term increases in intrinsic water-use efficiency do not lead to increased stem growth in a tropical monsoon forest in western Thailand. Glob Change Biol 17(2):1049–1063. https://doi.org/10.1111/j.1365-2486.2010.02222.x

Pacheco A, Camarero JJ, Carrer M (2016) Linking wood anatomy and xylogenesis allows pinpointing of climate and drought influences on growth of coexisting conifers in continental Mediterranean climate. Tree Physiol 36(4):502–512. https://doi.org/10.1093/treephys/tpv125

Pan Y, Birdsey RA, Fang J, Houghton R, Kauppi PE, Kurz WA, Phillips OL, Shvidenko A, Lewis SL, Canadell JG, Ciais P, Jackson RB, Pacala SW, McGuire AD, Piao S, Rautiainen A, Sitch S, Hayes D (2011) A large and persistent carbon sink in the world's forests. Science 333(6045):988–993. https://doi.org/10.1126/science.1201609

Pellizzari E, Camarero JJ, Gazol A, Sanguesa-Barreda G, Carrer M (2016) Wood anatomy and carbon-isotope discrimination support long-term hydraulic deterioration as a major cause of drought-induced dieback. Glob Change Biol 22(6):2125–2137. https://doi.org/10.1111/gcb.13227

Peñuelas J, Hunt JM, Ogaya R, Jump AS (2008) Twentieth century changes of tree-ring $\delta^{13}C$ at the southern range-edge of *Fagus sylvatica*: increasing water-use efficiency does not avoid the growth decline induced by warming at low altitudes. Glob Change Biol 14(5):1076–1088. https://doi.org/10.1111/j.1365-2486.2008.01563.x

Peñuelas J, Canadell JG, Ogaya R (2011) Increased water-use efficiency during the 20th century did not translate into enhanced tree growth. Glob Ecol Biogeogr 20(4):597–608. https://doi.org/10.1111/j.1466-8238.2010.00608.x

Puchi PF, Camarero JJ, Battipaglia G, Carrer M (2021) Retrospective analysis of wood anatomical traits and tree-ring isotopes suggests site-specific mechanisms triggering Araucaria araucana drought-induced dieback. Glob Chang Biol 27(24):6394–6408. https://doi.org/10.1111/gcb.15881

Rahman M, Islam M, Gebrekirstos A, Bräuning A (2019) Trends in tree growth and intrinsic water-use efficiency in the tropics under elevated CO2 and climate change. Trees 33(3):623–640. https://doi.org/10.1007/s00468-019-01836-3

Reich PB, Hobbie SE, Lee TD, Pastore MA (2018) Unexpected reversal of C3 versus C4 grass response to elevated CO2 during a 20-year field experiment. Science 360:317–320. https://doi.org/10.1126/science.aas9313

Rosseel Y (2012) lavaan: an R package for structural equation modeling. J Stat Softw 48(2):1–36. https://doi.org/10.18637/jss.v048.i02

Samusevich A, Lexa M, Vejpustková M, Altman J, Zeidler A (2020) Comparison of methods for the demarcation between earlywood and latewood in tree rings of Norway spruce. Dendrochronologia 60:125686. https://doi.org/10.1016/j.dendro.2020.125686

Saurer M, Siegwolf RTW, Schweingruber FH (2004) Carbon isotope discrimination indicates improving water-use efficiency of trees in northern Eurasia over the last 100 years. Glob Change Biol 10(12):2109–2120. https://doi.org/10.1111/j.1365-2486.2004.00869.x

Saurer M, Spahni R, Frank DC, Joos F, Leuenberger M, Loader NJ, McCarroll D, Gagen M, Poulter B, Siegwolf RT, Andreu-Hayles L, Boettger T, Dorado Liñán I, Fairchild IJ, Friedrich M, Gutierrez E, Haupt M, Hilasvuori E, Heinrich I, Helle G, Grudd H, Jalkanen R, Levanič T, Linderholm HW, Robertson I, Sonninen E, Treydte K, Waterhouse JS, Woodley EJ, Wynn PM, Young GH (2014) Spatial variability and temporal trends in water-use efficiency of European forests. Glob Chang Biol 20(12):3700–3712. https://doi.org/10.1111/gcb.12717

Schimel D, Stephens BB, Fisher JB (2015) Effect of increasing CO_2 on the terrestrial carbon cycle. Proc Natl Acad Sci USA 112(2):436–441. https://doi.org/10.1073/pnas.1407302112

Schneider L, Gärtner H (2013) The advantage of using a starch based non-Newtonian fluid to prepare micro sections. Dendrochronologia 31(3):175–178. https://doi.org/10.1016/j.dendro.2013.04.002

Sevanto S, McDowell NG, Dickman LT, Pangle R, Pockman WT (2014) How do trees die? A test of the hydraulic failure and carbon starvation hypotheses. Plant Cell Environ 37(1):153–161. https://doi.org/10.1111/pce.12141

Soulé PT, Knapp PA, Williams J (2015) Analyses of intrinsic water-use efficiency indicate performance differences of ponderosa pine and Douglas-fir in response to CO_2 enrichment. J Biogeogr 42(1):144–155. https://doi.org/10.1111/jbi.12408

Tyree MT, Zimmermann MH (2002) Xylem structure and the ascent of sap, 2nd, eds. Springer-Verlag, Berlin

Urrutia-Jalabert R, Malhi Y, Barichivich J, Lara A, Delgado-Huertas A, Rodríguez CG, Cuq E (2015) Increased water use efficiency but contrasting tree growth patterns in *Fitzroya cupressoides* forests of southern Chile during recent decades. J Geophys Res-Biogeosci 120(12):2505–2524. https://doi.org/10.1002/2015jg003098

Vaganov EA, Hughes MK, Shashkin AV (2006) Growth dynamics of conifer tree rings: images of past and future environments, 1st edn. Edn. Springer-Verlag, Berlin

Voelker SL, Brooks JR, Meinzer FC, Anderson R, Bader MK, Battipaglia G, Becklin KM, Beerling D, Bert D, Betancourt JL, Dawson TE, Domec JC, Guyette RP, Korner C, Leavitt SW, Linder S, Marshall JD, Mildner M, Ogee J, Panyushkina I, Plumpton HJ, Pregitzer KS, Saurer M, Smith AR, Siegwolf RT, Stambaugh MC, Talhelm AF, Tardif JC, de Van Water PK, Ward JK, Wingate L (2016) A dynamic leaf gas-exchange strategy is conserved in woody plants under changing ambient CO_2: evidence from carbon isotope discrimination in paleo and CO_2 enrichment studies. Glob Change Biol 22(2):889–902. https://doi.org/10.1111/gcb.13102

Wagner F, Rossi V, Stahl C, Bonal D, Herault B (2012) Water availability is the main climate driver of neotropical tree growth. PLoS One 7(4):e34074. https://doi.org/10.1371/journal.pone.0034074

Wang DX, Lin YY, Lei RD, Yang T, Wang Q, Yong XH (2009) Community composition and classification of natural forest of Chinese pine (*Pinus tabulaeformis* Carr.) in Qinling Mountains (in Chinese). Acta Bot Bor-Occid Sin 29(5):1016–1025

Wang Y, Zhang Y, Fang O, Shao X (2018) Long-term changes in the tree radial growth and intrinsic water-use efficiency of Chuanxi spruce (Picea likiangensis var: balfouriana) in southwestern China. J Geogr Sci 28(6):833–844. https://doi.org/10.1007/s11442-018-1508-7

Wang W, McDowell NG, Liu X, Xu G, Wu G, Zeng X, Wang G (2021) Contrasting growth responses of Qilian juniper (*Sabina przewalskii*) and Qinghai spruce (*Picea crassifolia*) to CO_2 fertilization despite common water-use efficiency increases at the northeastern

Qinghai-Tibetan plateau. Tree Physiol 41(6):992–1003. https://doi.org/10.1093/treephys/tpaa169

Wieser G, Oberhuber W, Waldboth B, Gruber A, Matyssek R, Siegwolf RTW, Grams TEE (2018) Long-term trends in leaf level gas exchange mirror tree-ring derived intrinsic water-use efficiency of *Pinus cembra* at treeline during the last century. Agric for Meteorol 248:251–258. https://doi.org/10.1016/j.agrformet.2017.09.023

Xu G, Liu X, Belmecheri S, Chen T, Wu G, Wang B, Zeng X, Wang W (2018) Disentangling contributions of CO_2 concentration and climate to changes in intrinsic water-use efficiency in the arid boreal forest in China's Altay Mountains. Forests 9(10):642–662. https://doi.org/10.3390/f9100642

Zhang J, Gou X, Manzanedo RD, Zhang F, Pederson N (2018) Cambial phenology and xylogenesis of Juniperus przewalskii over a climatic gradient is influenced by both temperature and drought. Agric for Meteorol 260–261:165–175. https://doi.org/10.1016/j.agrformet.2018.06.011